A river stage correction approach using Fourier series

Xiaoqin Zhang and Weimin Bao

ABSTRACT

One-dimensional hydrodynamic models based on the Saint-Venant equations (the SVN model) are used widely for river stage prediction. Errors that originate from simplifying assumptions, improper specification of initial and boundary conditions, uncertainty in parameters, channel geometry, observed data, and solution methods produce the inconsistencies between actual flow and that represented by the SVN model; this problem is especially apparent in tidal rivers. All of these simplifications and sources of imprecision can accumulate and introduce substantial errors in application. Total errors due to the causes mentioned above are treated as an error function, which is introduced as an additive term in the SVN model momentum equation. The function is constructed using a Fourier series approximation of discrepancies between simulated and observed flow. By combining the SVN model with the error function, a river stage correction approach (the ISV model) is proposed to take account of unconsidered errors in application. The tidal reach of the Qiantang River is selected as the study case and results based on a classification of flood events show that the ISV model generally performs better than the SVN model alone. It indicates that the approach could help guide improvements on the SVN model performance.

Key words | error function, Fourier series, river stage correction, tidal river

Xiaoqin Zhang (corresponding author)
Weimin Bao
College of Hydrology and Water Resources,
State Key Laboratory of Hydrology-Water,
Resources and Hydraulic Engineering,
Hohai University,
Nanjing, 210098,
China
E-mail: *zxqin403@163.com*

INTRODUCTION

Many hydrodynamic models are currently used to describe flow dynamics, including one-dimensional (1-D) models based on the Saint-Venant equations (e.g. Saavedra *et al.* 2003; Hsu *et al.* 2006), 2-D models based on the 2-D shallow water equations (e.g. Frison 2000; Lei *et al.* 2009), 3-D models based on the Navier-Stokes equations (e.g. Liu *et al.* 2007; Vaz *et al.* 2009) or certain other coupled models (e.g. Tayefi *et al.* 2007; Hu *et al.* 2009). Due to ease of use, low cost and generally robust performance, 1-D hydrodynamic models based on the Saint-Venant equations (the SVN model) are frequently used to handle flood routing problems.

The Saint-Venant equations are derived physically by applying the principles of mass and momentum conservation under a set of simplifying assumptions including smoothly changing flow, uniform velocity across a section, hydrostatic pressure distribution, friction for steady flow, small average bottom slope, horizontal transverse slope, and smooth curvature of the free surface (e.g. Saavedra *et al.* 2003), which are an incomplete description of flow process. In situations where some of these assumptions are not valid, the computed results may become unreliable (e.g. Chaudhry 2011). These assumptions are inconsistent with actual flow dynamics especially in rivers with significant tidal effects; the result of the application of these poor assumptions is a form of model structural error (Clark & Kavetski 2010). Flow dynamics in tidal rivers is complicated by the changes of incoming flow moving downstream and tide periodically propagating upstream or downstream. Tidal effects can significantly impact wave translation and attenuation (Sobey 2001); likewise tide propagation is affected by river discharge (e.g. Godin 1985; Horrevoets *et al.* 2004). Additionally, flow routing in tidal rivers imposed by tidal effects can produce large dynamic water pressure gradients, which are poorly modelled by the hydrostatic

doi: 10.2166/nh.2012.149

water pressure assumption. This factor is particularly a problem in certain scenarios such as tidal bores (e.g. Mazumder & Bose 1995) and coincidences of astronomical tide and storm surge. Manning's formula is commonly used to represent flow resistance (e.g. Yen 2001; Hsu *et al.* 2006); however, it is valid only for steady flow and thus may not provide realistic estimates, especially if improper roughness values are used. These errors – the results of simplifying assumptions and the incomplete model structure – are frequently neglected in practice. In addition, the SVN model is subject to errors due to improper specification of initial and boundary conditions, uncertainty in parameter values, channel geometry, local inflow estimation, and observed data, as well as techniques used to solve the partial differential equations (Butts *et al.* 2004; Guganesharajah *et al.* 2006). It is known that flow routing is affected greatly by channel geometric features and characteristics of sources and sinks. Tidal channels usually exhibit dramatic changes in morphology under interaction between incoming flow and tide (Chang 1997; Lee & Julien 2006). The roughness values can sometimes compensate for the model limitations in representing the effects of geometry, which cannot be directly measured but may lead to significant uncertainty (e.g. Johnson 1996; Pappenberger *et al.* 2006). All of these simplifications and sources of imprecision can accumulate and introduce substantial errors in the application of the SVN model despite our perfect knowledge of the governing laws.

Many methods have been employed to improve model performance, including state variable updating (e.g. Neal *et al.* 2007; Wu *et al.* 2008), parameter updating (e.g. Hsu *et al.* 2006; Bao *et al.* 2009) and error prediction (e.g. Madsen & Skotner 2005; Zhang *et al.* 2009), but little attention has been paid to the effect of unconsidered errors on the governing equations. Previous studies have derived error functions for the solution of approximations of the Saint-Venant equations by comparing its approximations to the dynamic wave solution (Singh 1994; Singh & Aravamuthan 1995). Constructing error functions to account for the effects of approximations of the Saint-Venant equations is an effective way to study the applicability of the approximations themselves under different conditions. However, it is difficult to evaluate and specify the difference between actual flow dynamics and that represented by the Saint-Venant equations affected by the simplifying assumptions and sources of imprecision mentioned, which needs further study.

This study aims to improve water stage predictions by taking accounting of the errors stemming from the unconsidered factors list above. Difficulty arises in attempting to decompose effects of errors from different sources, and this task is beyond the scope of this paper. In this study, the comprehensive errors are treated as a single error function included as a term in the momentum equation of the SVN model. By incorporating this function the improved momentum equation can comprehensively reflect errors contributed by the unconsidered factors in the application of the original SVN model. A Fourier series technique is used to construct the error function. In the study case the newly developed approach (referred to as the ISV model) that combines the SVN model with the error function is applied to correct river stage prediction in the tidal channel of the Qiantang River in China.

METHODS

Basic equations

The Saint-Venant equations are given as:

$$B\frac{\partial h}{\partial t}+\frac{\partial (Av)}{\partial x}=0 \tag{1}$$

$$\frac{\partial v}{\partial t}+v\frac{\partial v}{\partial x}+g\frac{\partial h}{\partial x}+g\frac{v|v|}{c^2R}=gS_0 \tag{2}$$

where v is the velocity, h is the flow depth, c is the Chezy coefficient, B is the channel width, A is the cross-sectional area, R is the hydraulic radius, x is the longitudinal distance, S_0 is the riverbed gradient and g is the gravitational acceleration, t is the independent variable of time.

The momentum equation combined with a general error function term is expressed as:

$$\frac{\partial v}{\partial t}+v\frac{\partial v}{\partial x}+g\frac{\partial h}{\partial x}+g\frac{v|v|}{c^2R}=gS_0+F_t \tag{3}$$

where F_t is the error function representing the error contributed by the factors that cannot be considered in the application of the SVN model.

In view of that the specific expression of F_t is unknown and any reasonable function can be decomposed into contributions from sine and cosine, Fourier series was adopted to construct the error function. The Fourier series expansion of F_t is expressed as:

$$F_t = \frac{a_0}{2} + \sum_{k=1}^{M} (a_k \cos \omega_k t + b_k \sin \omega_k t) \quad (4)$$

where ω_k is the angular frequency, M is the number of harmonic components, a_0, a_k and b_k are the Fourier coefficients.

By combining Equations (1), (3) and (4) the proposed method accounting for the errors unconsidered in the application of the SVN model is referred to as the ISV model.

Model solution

The classical four-point implicit Preissmann scheme is adopted to discretize the model equations. The calculation frame for the ISV model is shown in Figure 1. In the frame, e is the iteration number and h_{obs} represents the observed flow depth. In accordance with the frame, the specific calculation procedure is as follows.

- Step 1: Input the upstream and downstream boundary conditions into the SVN model. The flow velocity u_e and the flow depth h_e are calculated. The root mean square error (RMSE) between the h_e and the observations is computed, which is referred as RMSE_e. In this step, the value of e is set to 0.
- Step 2: Input the observed flow depth and the calculated velocity u_e into the Equation (3). The function F_t is calculated, and subsequently referred as F_e. The Fourier coefficients a_0, a_k and b_k can be directly calculated by using the least squares method.

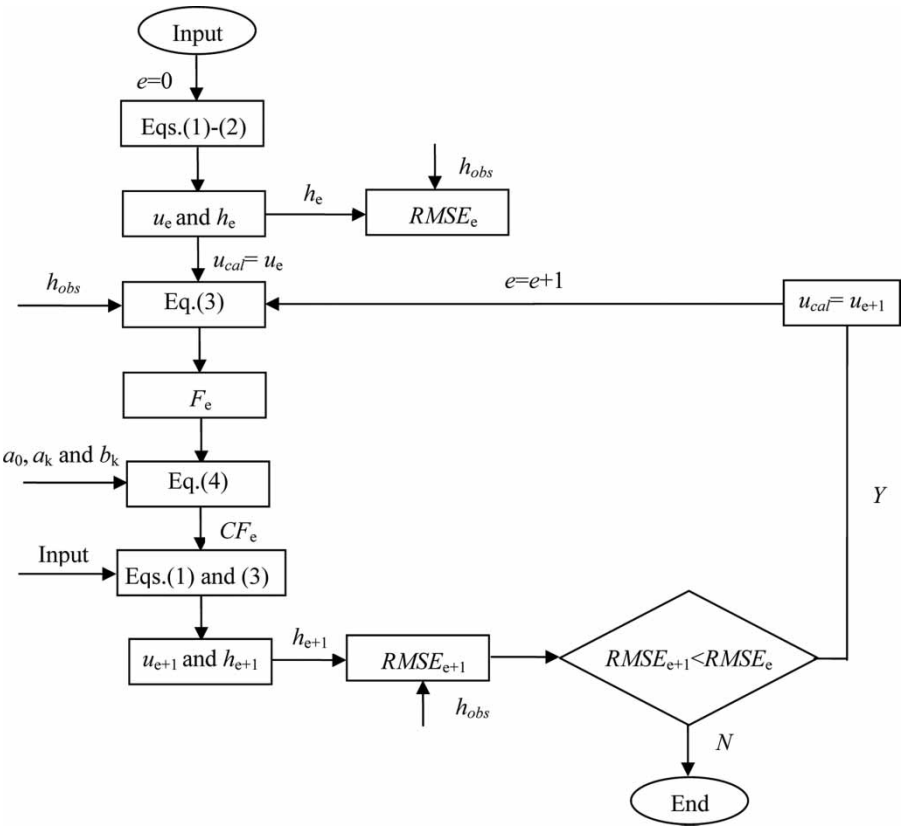

Figure 1 | Calculation frame for the ISV model.

- Step 3: With the calculated Fourier coefficients, the approximate representations of the function F_e are obtained. These are referred as CF_e.
- Step 4: Input the upstream and downstream boundary conditions and CF_e into Equations (1) and (3). The velocity u_{e+1} and flow depth h_{e+1} are calculated. The RMSE between the h_{e+1} and the observations is computed, which is referred as $RMSE_{e+1}$.
- Step 5: If $RMSE_{e+1} < RMSE_e$, go to Step 2; if not, the iteration process ends and the final optimized Fourier coefficients are obtained. The u_e and h_e are the final model solutions after e iterations.

The calculation procedure from Step 1 and iteratively Steps 2 through 5 is used to calculate Fourier coefficients. Step 5 is used to judge whether to continue the iteration process. With the successive iterations of Steps 1 through 5, the error function based on the Fourier series approximations can theoretically approach the actual representation of the errors caused by unconsidered factors. In the condition that if the Fourier coefficients are given *a priori*, perhaps having been calculated using historic floods, the model results can be calculated with a single iteration of Steps 1 and 4. In general there are only several stations with available observed flow data along a river. If observed water stages are available at p stations, we will obtain $(p-1)$ sets of F_e in Step 2 and $(p-1)$ sets of CF_e in Step 3 corresponding to the $(p-1)$ sub-channels divided by the stations. Because the number of stations with available observed flow data is generally less than that of cross-sections with surveyed channel geometry data, it is suggested that the CF_e in a sub-channel between neighboring stations be decomposed into several parts according to the sub-sub-channels divided by the cross-sections in a sub-channel in Step 4. We can average CF_e for each sub-sub-channel by using uniform weights or the weights estimated as the proportions of the sub-sub-channel lengths to the sub-channel length.

The estimation of the Fourier coefficients by using the least squares method involved in the calculation procedure above is shown below. The momentum equation combined with a general error function term shown in Equation (3) can be rewritten as:

$$F_t = \frac{\partial v}{\partial t} + v\frac{\partial v}{\partial x} + g\frac{\partial h}{\partial x} + g\frac{v|v|}{c^2 R} - gS_0 \tag{5}$$

The vector-matrix form of Fourier series expansion of F_t shown in Equation (4) can be expressed as:

$$Y = XC + E \tag{6}$$

where

$$X = \begin{bmatrix} 0.5 & \cos\omega_1 t_1 & \cos\omega_2 t_1 & \dots & \cos\omega_M t_1 \\ 0.5 & \cos\omega_1 t_2 & \cos\omega_2 t_2 & \dots & \cos\omega_M t_2 \\ \dots & \dots & \dots & & \dots \\ 0.5 & \cos\omega_1 t_l & \cos\omega_2 t_l & \dots & \cos\omega_M t_l \end{bmatrix} \times \begin{bmatrix} \sin\omega_1 t_1 & \sin\omega_2 t_1 & \dots & \cos\omega_M t_1 \\ \sin\omega_1 t_2 & \sin\omega_2 t_2 & & \cos\omega_M t_2 \\ \dots & \dots & & \dots \\ \sin\omega_1 t_l & \sin\omega_2 t_l & \dots & \cos\omega_M t_l \end{bmatrix};$$

l is the number of observations;

$$Y = \begin{bmatrix} F_1 \\ F_2 \\ \dots \\ F_l \end{bmatrix}; \quad C = [\, a_0 \quad a_1 \quad \dots \quad a_M \quad b_1 \quad \dots \quad b_M \quad]^T;$$

F_t is the calculated value of the Equation (5) with the observed flow depths and the calculated velocity by the SVN model; E is the error.

By using the least squares method with $\mathrm{Min}\{E^T E = (Y - XC)^T (Y - XC)\}$, the estimates of the Fourier coefficients are expressed as:

$$\hat{C} = (X^T X)^{-1} X^T Y \tag{7}$$

STUDY CASE

Study area and data

The Qiantang River is located at Zhejiang Province in China (Figure 2). It runs from west to east and discharges into the Hangzhou Bay, then into the East China Sea. The basin has

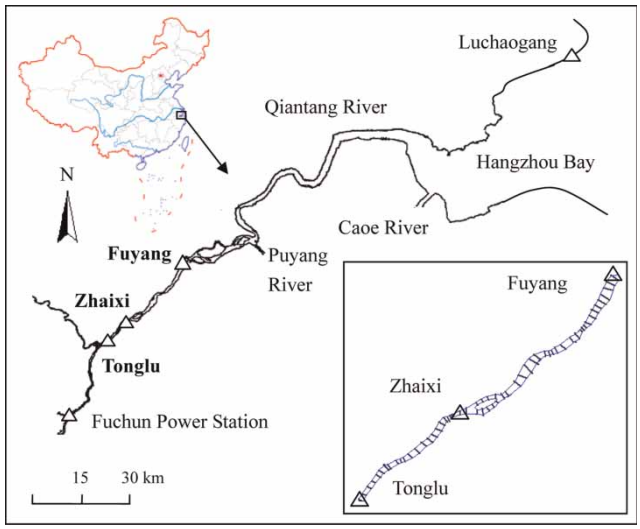

Figure 2 | Location of the study sites.

a subtropical monsoon climate, warm and humid with abundant precipitation. The Qiantang River Estuary is a typical strong tidal estuary. The astronomical tide in this estuary is of the irregular semi-diurnal kind. In the downstream funnel-shape Hangzhou Bay spectacular tidal bore forms (Su *et al.* 2001). In spring tide the tide can travel upstream to the Fuchun Power Station, 281 km from the mouth of the Hangzhou Bay (Pan *et al.* 2007). The tidal reach from the Tonglu station to Fuyang station is selected as the study channel (Figure 2). Tonglu is the upstream boundary controlled by river discharge and Fuyang is the downstream boundary affected by tide. The cross-sections along the river are of compound nature varying with different main channels and floodplains. Fifty cross-sections were surveyed along the study channel including those at the Tonglu, Zhaixi, and Fuyang hydrologic stations. It is about 15.6 km between Tonglu and Zhaixi, and about 28.6 km from Zhaixi to Fuyang. Fifty five flood events during the years 1981–1989 are collected to simulate river stages at Zhaixi.

Model application

The estimation of the angular frequency ω_k in Equation (4) is important; it should reflect the characteristics of the unconsidered factors that contributed to the error function F_t. Considering that flow in the study reach is affected by tide, we estimate the ω_k according to the angle velocity of tidal constituents. More tidal constituents considered can theoretically lead better agreement between F_t and its Fourier series approximation; however the calculation process can be very time consuming. For practicality, 11 primary tidal components are considered which can account for the main tidal effects, including the principal semi-diurnal ones, M_2, S_2, N_2, K_2, the principal diurnal ones, K_1, O_1, P_1, Q_1, and the compound ones due to topography and effect of interference, M_4, M_6, MS_4.

The flood events in the study case display different characteristics, parts of which are controlled by river flow while others are tidal. Noticeable differences exist between the Fourier coefficients for these different event classes. We can classify these historical flood events to better represent different flow conditions. According to the relative effect of upstream flow and downstream tide, 55 events are simply divided into 18 events controlled by river flow and 37 events dominated by tide. The events in each class are split into two parts respectively for model calibration and validation, that is, 25 of 37 tide-dominated events for calibration and 12 for validation, and 10 of 18 river-flow-controlled events for calibration and eight for validation. The events of each class for calibration are respectively treated as a whole time series to calculate the values of a_0, a_k and b_k by using the least squares method.

Due to the difficulty of describing the structure of the error function, the approach of Fourier expansion provides a possible way to approximate the error function. To show the characteristics of the errors, the time-series plots and hydrographs of the error function F_t in one section and the water depth error E_h between observations and calculations at Zhaixi for one flood event are respectively displayed in Figures 3 and 4. From Figures 3 and 4, it can be seen that the error function F_t values correlate well with the water depth errors; this situation indicates that it is feasible to assume a unique error function of time.

Hourly water stage observations are available, thus the time step is set to 1 hour. The weighting parameter 'theta' of the classical four-point implicit Preissmann scheme is estimated as 0.95. The relative error of simulated and observed peak stages (RPSE), RMSE, Nash-Sutcliffe efficiency (CE), and relative effective coefficient (DR) are calculated at the forecasted station to compare the performance of the ISV and SVN models in terms of stage

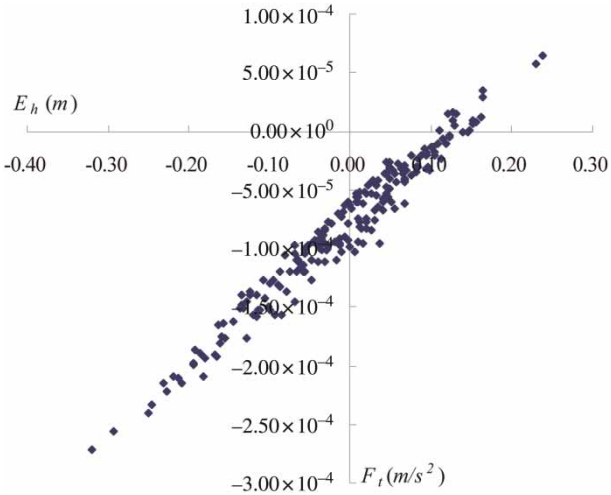

Figure 3 | Time-series plots between the F_t and E_h for Flood 820523.

simulation. They are calculated as:

$$\text{RPSE} = \frac{ZC_{\max} - Z_{\max}}{Z_{\max}} \times 100\% \tag{8}$$

$$\text{RMSE} = \sqrt{\frac{\sum_{i=1}^{N} (Z_i - ZC_i)^2}{N}} \tag{9}$$

$$\text{CE} = 1 - \frac{\sum_{i=1}^{N} [Z_i - ZC_i]^2}{\sum_{i=1}^{N} [Z_i - \overline{Z}]^2} \tag{10}$$

$$\text{DR} = 1 - \sum_{i=1}^{N} (ZC_{2,i} - Z_i)^2 \Big/ \sum_{i=1}^{N} (ZC_{1,i} - Z_i)^2 \tag{11}$$

where $Z_{\max}$ and $ZC_{\max}$ respectively represent the observed and calculated peak stage, Z_i and ZC_i respectively represent the observed and calculated stage at the time of i, $\overline{Z}$ is the average observed stage, $ZC_{1,i}$ and $ZC_{2,i}$ respectively represent the stage calculated by the SVN model and the ISV model at the time of i, and N is the total number of the observations for one flood event. A larger positive value of DR indicates increasingly better performance by the ISV model than the SVN model.

RESULTS

From the tests according to the calculation frame in Figure 1, it is found that the ISV simulations can converge to the final optimized results in less than 10 iterations of Steps 1 through 5 and represent a slight improvement over the results obtained by using only Steps 1 through 4. Tables 1–4 respectively list the results that are obtained by using the ISV model Steps 1 through 4 and the SVN model for the events controlled by river flow and those dominated by tidal effects at Zhaixi in the Qiantang River. Selected measured and modelled stage hydrographs are compared in Figures 5–8.

From the calibrated results for the river-flow-controlled events in Table 1, the ISV model performs better than the SVN model. Compared with the SVN model, the ISV improvements increase the average Nash-Sutcliffe efficiency (CE) from 0.912 to 0.940 and reduce the average RMSE from 0.296 to 0.233 m. The relative effective coefficient

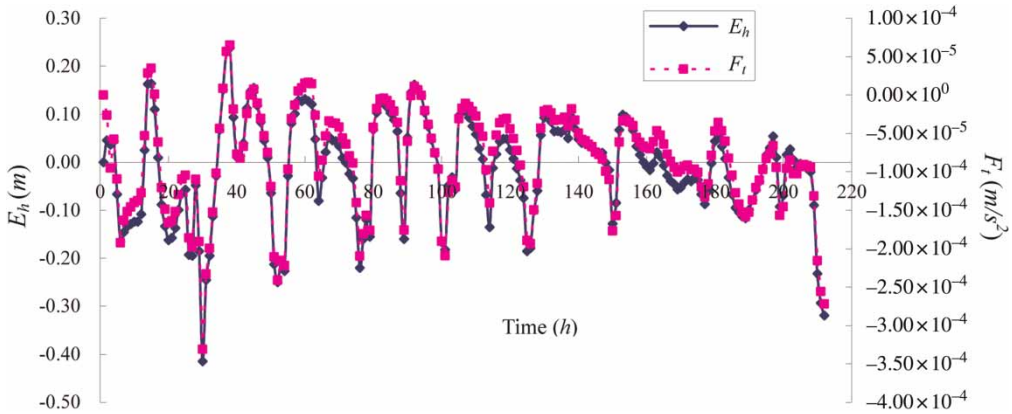

Figure 4 | Hydrographs of the F_t and E_h for Flood 820523.

Table 1 | Calibrated results for river-flow-controlled events at Zhaixi in the Qiantang River

			RPSE (%)		RMSE (*m*)		CE		
Flood event	**Occurrence time**	Z_{max} (*m*)	**ISV**	**SVN**	**ISV**	**SVN**	**ISV**	**SVN**	**DR**
810401	1–10 April 1981	10.75	–0.03	–1.95	0.121	0.176	0.987	0.974	0.500
811101	1–11 November 1981	9.23	–2.65	–5.22	0.185	0.294	0.943	0.856	0.604
820218	18–27 February 1982	8.33	–0.82	–3.18	0.182	0.198	0.949	0.941	0.135
820512	12–18 May 1982	7.42	–0.63	–3.78	0.161	0.180	0.832	0.791	0.196
820617	17–26 June 1982	12.73	–2.04	–3.38	0.212	0.257	0.986	0.979	0.333
830409	9–24 April 1983	12.09	–1.65	–3.25	0.138	0.224	0.988	0.969	0.612
830612	12 June to 4 July 1983	12.50	–1.90	–3.63	0.268	0.305	0.972	0.963	0.243
830704	4–22 July 1983	13.11	–3.32	–4.67	0.375	0.522	0.971	0.944	0.482
830915	15–24 September 1983	9.03	–8.14	–10.36	0.427	0.468	0.815	0.778	0.166
840607	7–18 June 1984	11.16	–4.27	–5.90	0.259	0.340	0.957	0.926	0.418
Average		10.64	–2.55	–4.53	0.233	0.296	0.940	0.912	0.369

Table 2 | Validated results for river-flow-controlled events at Zhaixi in the Qiantang River

			RPSE (%)		RMSE (*m*)		CE		
Flood event	**Occurrence time**	Z_{max} (*m*)	**ISV**	**SVN**	**ISV**	**SVN**	**ISV**	**SVN**	**DR**
870619	19–27 June 1987	11.46	–1.38	–2.66	0.227	0.245	0.980	0.977	0.130
870723	23–31 July 1987	10.49	–4.02	–5.43	0.377	0.478	0.877	0.803	0.375
880326	26 March to April 1 1988	9.70	1.05	–1.24	0.240	0.305	0.955	0.929	0.366
880508	8–15 May 1988	9.92	–0.07	–1.68	0.191	0.210	0.953	0.943	0.175
880617	17–26 June 1988	12.01	–2.55	–4.10	0.225	0.261	0.977	0.969	0.258
890527	27–31 May 1989	11.57	–0.81	–2.36	0.195	0.212	0.984	0.981	0.157
890617	17–21 June 1989	10.96	–0.93	–2.77	0.174	0.210	0.978	0.968	0.312
890628	28 June to 16 July 1989	13.02	–1.92	–3.59	0.355	0.427	0.978	0.968	0.312
Average		11.14	–1.33	–2.98	0.248	0.294	0.960	0.942	0.261

(DR) values are all positive with an average of 0.369 and a maximum of 0.612. The relative errors of simulated and observed peak stages (RPSE) for the ISV model are all lower than those for the SVN model. The average RPSE is 2.55% for the ISV model and 4.53% for the SVN model. The validated results in Table 2 also show that the simulations are improved by using the ISV model, the average RMSE reduced to 0.248 m from 0.294 m and the average CE increased to 0.960 from 0.942. The RPSE values for the ISV model are all lower than those for the SVN model. The DR values are all positive with an average of 0.261 and a maximum of 0.375. The stage hydrographs for calibration in Figure 5 and those for validation in Figure 6 show that the stages calculated by the ISV model can better capture high flows than the SVN model.

From the calibrated results for the tide-dominated events in Table 3, the ISV model generally produces better results than the SVN model. The ISV simulations have lower RMSE and higher CE than the SVN results. The DR values are all positive with a mean of 0.294 and a maximum of 0.612. As shown in Table 4, the validation results obtained by the ISV model are in good agreement with the observed data; the average RPSE, RMSE and CE for the ISV model are respectively 1.00%, 0.183 m and 0.861.

Table 3 | Calibrated results for tide-dominated events at Zhaixi in the Qiantang River

			RPSE (%)		RMSE (*m*)		CE		
Flood event	**Occurrence time**	Z_{max} (*m*)	**ISV**	**SVN**	**ISV**	**SVN**	**ISV**	**SVN**	**DR**
810204	4–16 February 1981	6.51	–2.62	–0.92	0.090	0.143	0.861	0.658	0.593
810216	16–28 February 1981	7.68	–1.95	–0.64	0.081	0.094	0.977	0.969	0.258
810602	2–11 June 1981	6.93	–2.01	0	0.124	0.150	0.902	0.857	0.314
810914	14–23 September 1981	7.20	–1.63	0.14	0.108	0.118	0.890	0.869	0.160
820523	23 May to 1 June 1982	6.83	0.98	2.85	0.106	0.171	0.945	0.858	0.612
820602	2–11 June 1982	7.17	–4.25	–2.43	0.160	0.184	0.769	0.694	0.245
821205	5–22 December 1982	6.89	–0.56	1.09	0.122	0.143	0.860	0.808	0.270
830113	13–24 January 1983	7.05	–2.02	–0.57	0.169	0.171	0.867	0.864	0.022
840314	14 March to 10 April 1984	10.62	–2.37	–1.09	0.285	0.331	0.935	0.913	0.252
840508	8–25 May 1984	9.04	–9.43	–8.26	0.273	0.323	0.902	0.864	0.279
841207	7–13 December 1984	6.61	–3.11	–1.27	0.108	0.119	0.810	0.768	0.181
850305	5–18 March 1985	8.95	–2.01	–0.95	0.267	0.289	0.911	0.895	0.152
850413	13–30 April 1985	7.28	–4.56	–2.60	0.174	0.227	0.855	0.752	0.415
850511	11–23 May 1985	7.98	–1.49	0.14	0.241	0.300	0.877	0.810	0.352
850602	2–13 June 1985	8.05	–1.15	0.07	0.259	0.265	0.879	0.873	0.047
851012	12–24 October 1985	7.28	–0.08	1.21	0.116	0.139	0.928	0.896	0.307
851205	5–21 December 1985	7.45	–1.36	0.07	0.123	0.149	0.903	0.860	0.307
860314	14–24 March 1986	8.08	–1.89	–0.10	0.095	0.116	0.929	0.894	0.330
860401	1–20 April 1986	9.68	–0.64	1.03	0.143	0.150	0.977	0.975	0.079
860509	9–18 May 1986	7.03	–1.73	0.09	0.138	0.196	0.862	0.721	0.505
860618	18–30 June 1986	8.39	–0.24	1.41	0.173	0.193	0.918	0.899	0.188
860704	4–18 July 1986	8.13	–3.26	–1.70	0.245	0.332	0.892	0.801	0.457
860818	18–31 August 1986	7.23	0.05	1.66	0.202	0.262	0.813	0.686	0.404
861110	10–28 November 1986	7.57	–1.44	0	0.159	0.197	0.871	0.802	0.348
861208	8–21 December 1986	6.88	–6.20	–4.77	0.138	0.163	0.755	0.660	0.279
Average		7.70	–2.20	–0.62	0.164	0.197	0.884	0.826	0.294

The maximum value of DR is up to 0.689. Although the peak stage errors for most events by using the ISV model are not improved, the RPSE values for 23 out of 25 events in the calibration and all events in the validation are less than 5%. From Figures 7 and 8, the stages simulated by the ISV model generally agree better with the observations than those by the SVN model.

In light of the simulations in the Qiantang River it can be concluded that the ISV model can produce better performance than the SVN model. It also indicates that the approach of constructing an error function term by using Fourier series in the SVN model momentum equation is effective to improve water stage predictions by accounting for errors caused by the simplifications in the Saint-Venant assumptions as well as poor data and parameterization in application.

DISCUSSION

The simplifications and sources of imprecision mentioned can produce the inconsistencies between actual flow and that represented by the SVN model. This study proposed an error correction approach using Fourier series to account

Table 4 | Validated results for tide-dominated events at Zhaixi in the Qiantang River

			RPSE (%)		RMSE (*m*)		CE		
Flood event	**Occurrence time**	Z_{max} (*m*)	**ISV**	**SVN**	**ISV**	**SVN**	**ISV**	**SVN**	**DR**
870214	14–18 February 1987	6.46	–2.38	–0.21	0.081	0.082	0.904	0.901	0.030
870510	10–25 May 1987	7.55	–0.03	1.60	0.229	0.285	0.817	0.717	0.353
870904	4–20 September 1987	10.08	–1.40	–0.14	0.276	0.335	0.955	0.933	0.328
871006	6–11 October 1987	7.93	–1.57	0.19	0.178	0.231	0.842	0.735	0.403
871208	8–20 December 1987	7.05	–1.25	0.38	0.165	0.167	0.854	0.850	0.026
880207	7–16 February 1988	6.71	–0.21	1.43	0.084	0.152	0.914	0.723	0.689
880418	18–26 April 1988	7.02	–0.63	0.85	0.133	0.174	0.917	0.859	0.411
880530	30 May to 10 June 1988	7.37	–1.26	0.58	0.210	0.273	0.798	0.660	0.405
880708	8–24 July 1988	7.12	–1.14	0.47	0.274	0.299	0.686	0.624	0.164
880922	22–30 September 1988	8.40	–0.76	0.45	0.227	0.283	0.922	0.879	0.355
881008	8–17 October 1988	6.81	–0.17	1.74	0.118	0.187	0.897	0.742	0.600
890818	18–25 August 1989	7.44	–1.22	0.55	0.226	0.266	0.823	0.756	0.274
Average		7.50	–1.00	0.66	0.183	0.228	0.861	0.782	0.337

for errors due to unconsidered factors in the SVN model applications. The approach does not require any information of the specific sources or structures of these unconsidered errors. In the case the best results of the ISV simulations are obtained in less than 10 iterations by using the RMSE as the objective function, which perform slightly better over the results obtained using only Steps 1 through 4; this finding indicates that the Fourier coefficients of the error function can quickly converge. Additionally, the ISV simulations that are obtained by using only Steps 1 through 4 exhibit noticeable improvement over the results by the SVN model; this implies the good capability of the error correction approach. Due to its good performance and ease of use, the ISV model with Steps 1 through 4 can be used for flow simulation in practical applications.

The number of harmonic components M and the frequency parameters ω can directly affect the calculation of the Fourier coefficients. To some extent the uncertainty in the corrected simulations arises mainly due to the approximation of the error function, which is affected by the estimates of M and ω. The ω in the study case is simply evaluated according to tidal flow characteristics. Other methods should be tried for different flow conditions, for example, $\omega_k = k\pi/l$, where l can be set as the half number of observations of a flood event to represent common conditions or the tidal period (around 12.5 hours) to reflect tidal river flow. One can notice that the peak stage simulations for some tide-dominated events calculated by the ISV model in Tables 3 and 4 are not improved compared with those by the SVN model. Considering some other tidal components or ω_k, we found that the RPSE for some floods with the ISV model can be reduced. It is possible to set some rules for the estimation of M, which may make the estimation easier. For a specific study case, we can set large number of M to calculate the Fourier coefficients a_0, a_k and b_k, and then compare the contribution of each harmonic component to choose the important components. Due to ease of use, the least squares method was employed to calculate Fourier coefficients in the case. In further works, the usage of the non-linear least squares method for estimating Fourier coefficients, the selection of ω and M from tests performed on specific river conditions, and the probabilistic predictions and uncertainty analysis will be studied.

The Fourier coefficients of the error function commonly vary over different floods representing different error characteristics. For floods with similar characteristics we can use the same error function; however if floods exhibit obvious different characteristics, it is better to analyze each event class with different error function. The floods

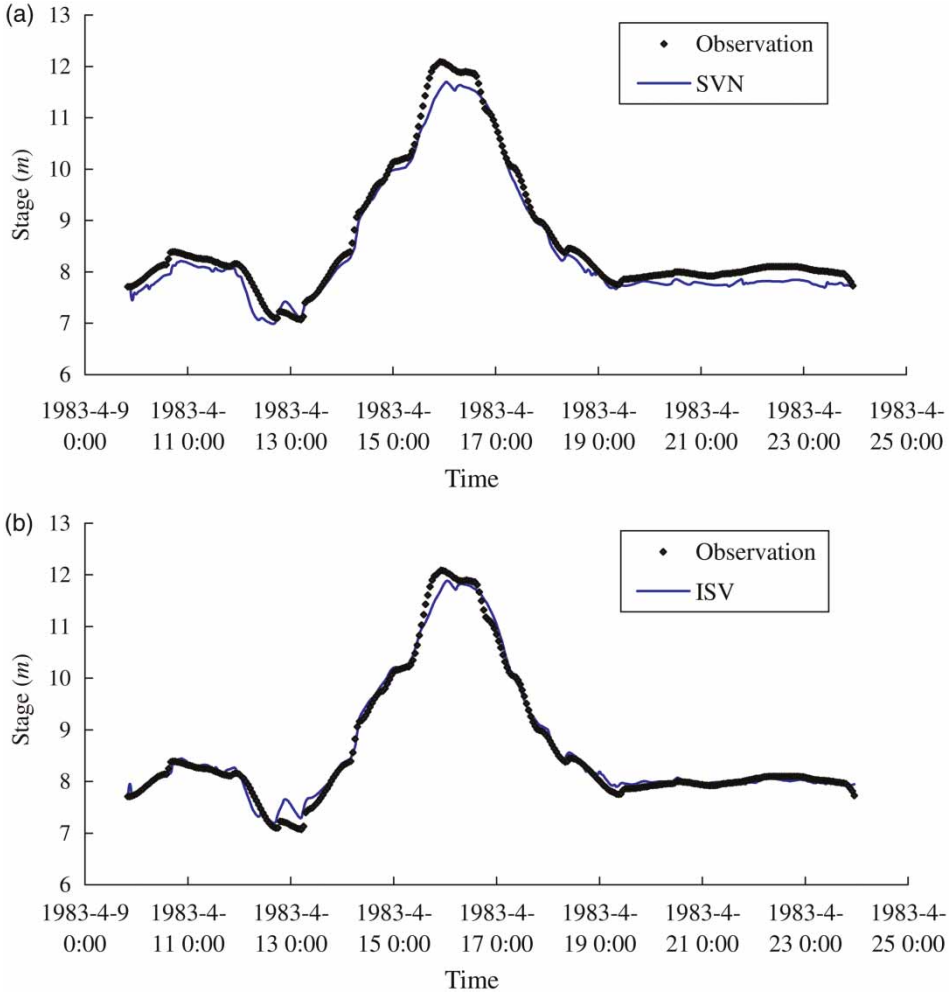

Figure 5 | Hydrographs of flood 830409 at Zhaixi in the Qiantang River. (a) Observation versus SVN model; (b) Observation versus ISV model.

in the study case are divided into two classes to represent different flow conditions; and the same ω_k are considered in each class. We can set some indexes for flood classification, which can reduce the uncertainty associated with choosing the class for a particular flood incident. Various methods have been developed for flood classification in literatures, such as artificial neural network, projection pursuit and fuzzy clustering algorithm, which can be employed to classify flood events in tidal rivers. We also can adjust ω_k for each class to better capture error characteristics. In this way the Fourier coefficients for each class would be best suitable for the corresponding type events, and the error functions would represent the particular error sources inherent in each type. From an operational point of view it would be useful to adopt the error correction approach for adjusting model forecasting results in a real-time system.

Theoretically, the poorer performance of the SVN model means that larger errors exist in its application, suggesting great potential to improve results by including an error correction technique, and vice versa. Considering complex flow dynamics in tidal rivers, we apply the ISV model for flow simulation in a tidal river in the case study to illuminate better the performance of the proposed approach. In the case the observed water stages are available only at three stations including Tonglu, Zhaixi and Fuyang, and the observations and simulations are compared only at Zhaixi. Conceptually, the introduction of the error

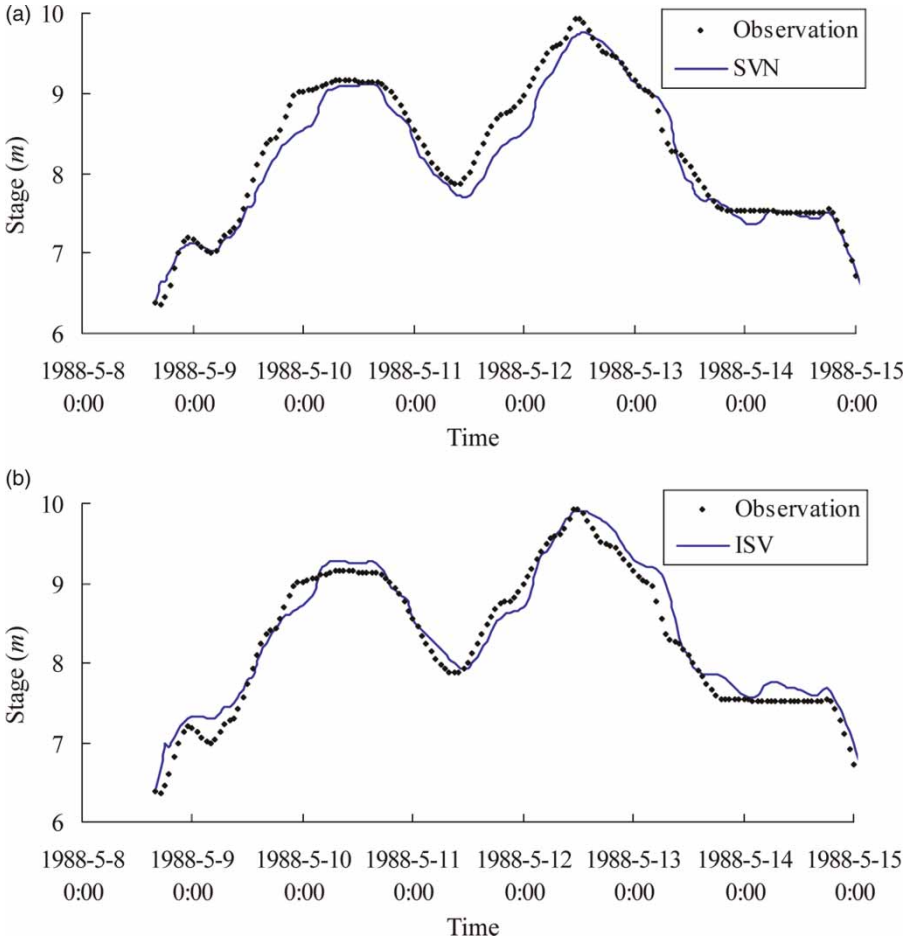

Figure 6 | Hydrographs of flood 880508 at Zhaixi in the Qiantang River. (a) Observation versus SVN model; (b) Observation versus ISV model.

function can yield an improvement on simulations at the cross-sections along the study river. With the increasing number of the cross-sections with available observations, more information can be used to express the error function. Meanwhile more attention should be paid to some problems, such as the data quality and computation. In a non-tidal river, there also exist unconsidered errors in SVN model application, such as roughness parameters uncertainty, channel geometry changing, etc. From the smooth change of the observations shown in Figures 3 and 4, it can be seen that the flow characteristics of the river-flow-controlled events are similar to those of events in a non-tidal river. It is also found that the error function F_t values correlate well with the water depth errors E_h for river-flow-controlled events. To some extent the good results calculated by the ISV model for river-flow controlled events can reflect its effective performance in non-tidal rivers. In further works, we will collect data to validate the reliability of the approach at other cross-sections along rivers and in non-tidal channels.

Another legitimate objective of using the error correction approach would establish relationships between the error function and its causes, which could help guide improvements on the model structure. There are significant obstacles for establishing such relationships, because the information contributed by all error sources is compressed into a single function, which yields only a single error term at any given time, and there may be an interaction between error sources. But it may be possible, with further study, to exclude certain error sources and analyze the resulting error function under highly controlled scenarios. Conceptually, if errors due to parameters and boundary and initial

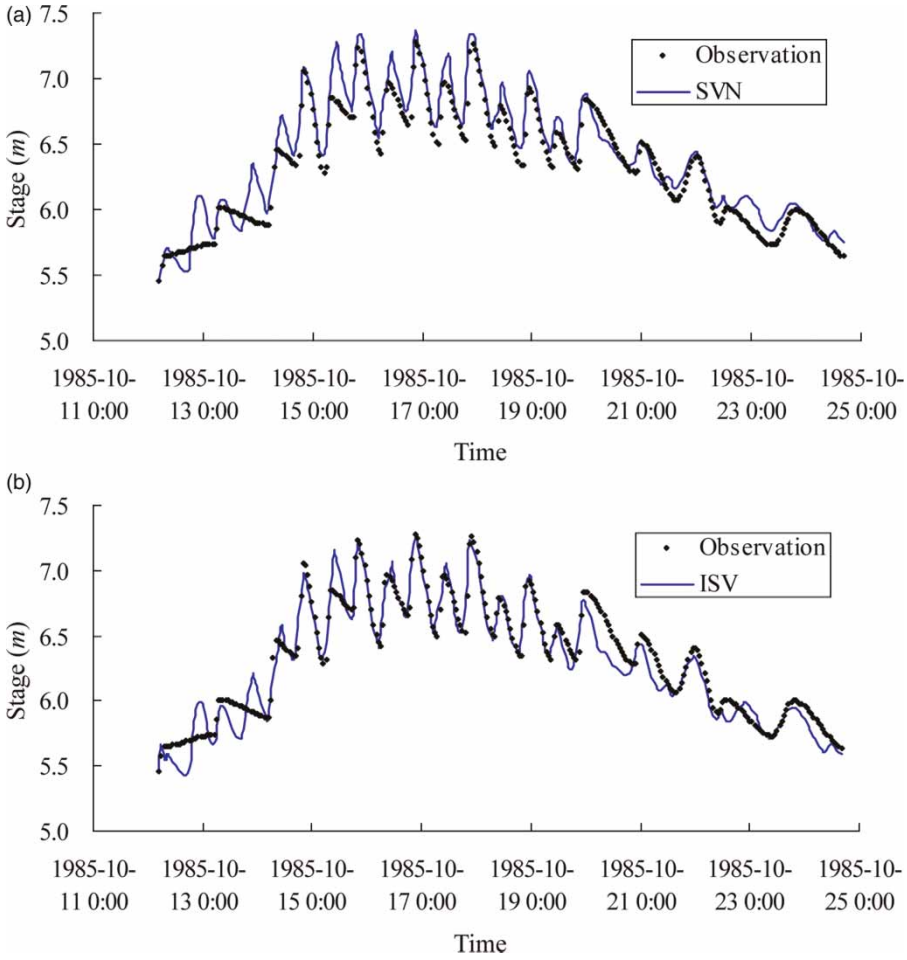

Figure 7 | Hydrographs of flood 851012 at Zhaixi in the Qiantang River. (a) Observation versus SVN model; (b) Observation versus ISV model.

conditions can be ignored in highly controlled conditions, the error function would mainly account for errors stemming from the model simplifying assumptions; if flow dynamics in a river are in accordance with the assumptions and appropriate boundary and initial conditions are used, the error function may be mainly caused by roughness parameters. From this perspective, the error correction approach would provide a useful tool for analyzing the relationship between manifest errors and related factors.

In tidal rivers tidal effects have significant impact on flood routing. The gravity, friction and water pressure are considered as the main driving forces in the Saint-Venant equations, and tidal effects are not considered directly in the equation derivation other than by using the downstream boundary conditions in its application. It is controversial whether the downstream boundary or the water pressure gradient in the SVN model can completely reflect tidal effects. In other words, there are questions about whether tidal effects introduce errors in the SVN model application in tidal rivers. The proposed error correction approach can be used to seek relationships between the error function and tidal effects. More works in this area are needed.

In general, the error correction approach with Fourier series potentially has the capability to improve model performance by incorporating error functions into partial differential equations. It provides a simple and possible way to effectively account for the comprehensive errors due to unconsidered factors in model applications. In theory, the approach could be extended to consider errors in the application of 2-D and 3-D hydrodynamic models based on partial differential equations, as well as models consisting of partial differential equations in other fields.

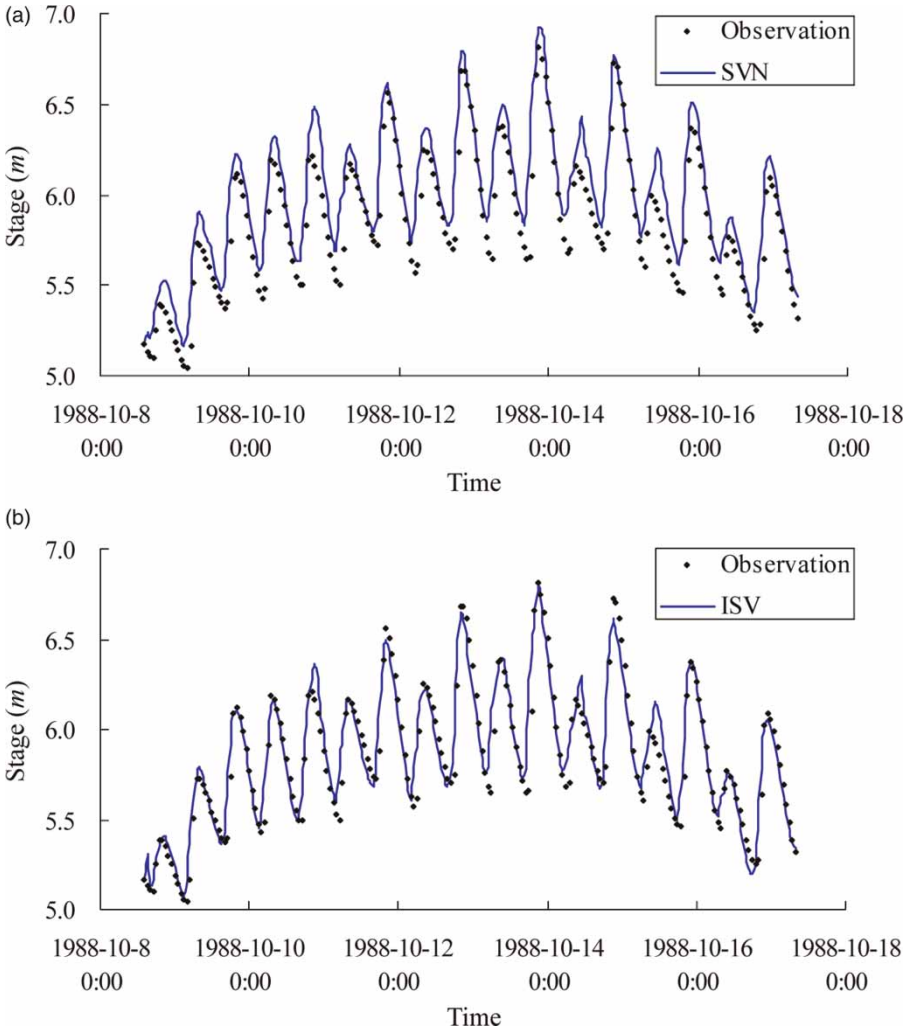

Figure 8 | Hydrographs of flood 881008 at Zhaixi in the Qiantang River. (a) Observation versus SVN model; (b) observation versus ISV model.

SUMMARY AND CONCLUSIONS

The errors that originate from various aspects of the application of the SVN model, including simplifying assumptions, improper specification of initial and boundary conditions, uncertainty in parameters, channel geometry, local inflow, observed data, and solution methods, can significantly affect model performance. In this study, an error correction approach using Fourier series was explored to approximate the comprehensive errors due to the unconsidered factors in the application of the SVN model. The results of the study are encouraging; they show that the proposed ISV model which combines the SVN model and the error correction approach can generally obtain better results than the SVN model alone. The proposed error correction approach is seen to be an effective way to represent the unconsidered errors in the SVN model applications. The approach can be used not only to improve the performance of the SVN model, but it also suggests a simple way to construct a specific expression of the error function caused by the unconsidered parts included in model applications.

The present study represents an initial effort; it demonstrates the performance of the error correction approach by application to a tidal river. A larger and more accurate data set is required to verify its capability in other rivers.

More attention should be paid to the selection of the angular frequency and the number of harmonic components in the Fourier series approximation of the error function. Furthermore, more works are needed to derive relationships between the error function and specific error causes, which could lead to an investigation of model structure and ultimately enhance model performance. In further studies we will focus on the errors in SVN model applications caused by tidal effects, which may extend our understanding of flow dynamics in tidal rivers.

ACKNOWLEDGEMENTS

The study was supported by the Fundamental Research Funds for the Central Universities (No. 2012B00214) and the National Natural Science Foundation of China (Grant No. 51279057). Thanks to the editor and anonymous reviewers for their helpful comments and suggestions, which improved the quality of the article.

REFERENCES

Bao, W. M., Zhang, X. Q. & Qu, S. M. 2009 Dynamic correction of roughness in the hydrodynamic model. *Journal of Hydrodynamics* **21**, 255–263.

Butts, M. B., Payne, J. T., Kristensen, M. & Madsen, H. 2004 An evaluation of the impact of model structure on hydrological modelling uncertainty for streamflow simulation. *Journal of Hydrology* **298** (1–4), 242–266.

Chang, H. H. 1997 Modeling fluvial processes in tidal inlet. *Journal of Hydraulic Engineering* **123**, 1161–1165.

Chaudhry, M. H. 2011 Modeling of one-dimensional, unsteady, free-surface, and pressurized flows. *Journal of Hydraulic Engineering* **137**, 148–157.

Clark, M. P. & Kavetski, D. 2010 Ancient numerical daemons of conceptual hydrological modeling: 1. Fidelity and efficiency of time stepping schemes. *Water Resources Research* **46**, W10510.

Frison, T. W. 2000 Dynamics of the residuals in estuary water levels. *Physics and Chemistry of the Earth, Part B: Hydrology, Oceans and Atmosphere* **25**, 359–364.

Godin, G. 1985 Modification of river tides by the discharge. *Journal of Waterway, Port, Coastal and Ocean Engineering* **111**, 257–274.

Guganesharajah, K., Lyons, D. J., Parsons, S. B. & Lloyd, B. J. 2006 Influence of uncertainties in the estimation procedure of floodwater level. *Journal of Hydraulic Engineering* **132**, 1052–1060.

Horrevoets, A. C., Savenije, H. H. G., Schuurman, J. N. & Graas, S. 2004 The influence of river discharge on tidal damping in alluvial estuaries. *Journal of Hydrology* **294**, 213–228.

Hsu, M. H., Fu, J. C. & Liu, W. C. 2006 Dynamic routing model with real-time roughness updating for flood forecasting. *Journal of Hydraulic Engineering* **132**, 605–619.

Hu, K. L., Ding, P. X., Wang, Z. B. & Yang, S. L. 2009 A 2D/3D hydrodynamic and sediment transport model for the Yangtze Estuary, China. *Journal of Marine System* **77** (1–2), 114–136.

Johnson, P. A. 1996 Uncertainty of hydraulic parameters. *Journal of Hydraulic Engineering* **122**, 112–114.

Lee, J. S. & Julien, P. Y. 2006 Downstream hydraulic geometry of alluvial channels. *Journal of Hydraulic Engineering* **132**, 1347–1352.

Lei, Z. Y., Zhang, J. H. & Kong, J. 2009 Numerical simulation of water level under interaction between runoff and estuarine dynamic in tidal reach of the Yangtze River. *China Ocean Engineering* **23**, 543–551.

Liu, W. C., Hsu, M. H. & Kuo, A. Y. 2007 Three-dimensional hydrodynamic and salinity transport modelling of Danshuei River estuarine system and adjacent coastal sea, Taiwan. *Hydrological Processes* **21**, 3057–3071.

Madsen, H. & Skotner, C. 2005 Adaptive state updating in real-time river flow forecasting-a combined filtering and error forecasting procedure. *Journal of Hydrology* **308** (1–4), 302–312.

Mazumder, N. C. & Bose, S. 1995 Formation and propagation of tidal bore. *Journal of Waterway, Port, Coastal, and Ocean Engineering* **121**, 167–175.

Neal, J. C., Atkinson, P. M. & Hutton, C. W. 2007 Flood inundation model updating using an ensemble Kalman filter and spatially distributed measurements. *Journal of Hydrology* **336** (3–4), 401–415.

Pan, C. H., Lin, B. Y. & Mao, X. Z. 2007 Case study: numerical modeling of the tidal bore on the Qiantang River, China. *Journal of Hydraulic Engineering* **133**, 130–138.

Pappenberger, F., Matgen, P., Beven, K. J., Henry, J. B., Pfister, L. & Fraipont, de P. 2006 Influence of uncertain boundary conditions and model structure on flood inundation predictions. *Advances in Water Resources* **29**, 1430–1449.

Saavedra, I., López, J. L. & García-Martínez, R. 2003 Dynamic wave study of flow in tidal channel system of San Juan River. *Journal of Hydraulic Engineering* **129**, 519–526.

Singh, V. P. 1994 Accuracy of kinematic wave and diffusion wave approximations for space-independent flows. *Hydrological Processes* **8**, 45–62.

Singh, V. P. & Aravamuthan, V. 1995 Accuracy of kinematic wave and diffusion wave approximations for time-independent flows. *Hydrological Processes* **9**, 755–782.

Sobey, R. J. 2001 Evaluation of numerical models of flood and tide propagation in channels. *Journal of Hydraulic Engineering* **127**, 805–823.

Su, M. D., Xu, X., Zhu, J. L. & Hon, Y. C. 2001 Numerical simulation of tidal bore in Hangzhou Gulf and Qiantangjiang. *International Journal for Numerical Methods in Fluids* **36**, 205–247.

Tayefi, V., Lane, S. N., Hardy, R. J. & Yu, D. 2007 A comparison of one- and two-dimensional approaches to modelling flood inundation over complex upland floodplains. *Hydrological Processes* **21**, 3190–3202.

Vaz, N., Dias, J. M. & Leitão, P. C. 2009 Three-dimensional modeling of a tidal channel: the Espinheiro Channel (Portugal). *Continental Shelf Research* **29**, 29–41.

Wu, X. L., Wang, C. H., Chen, X. & Xiang, X. H. 2008 Kalman filtering correction in real-time forecasting with hydrodynamic model. *Journal of Hydrodynamics* **20**, 391–397.

Yen, B. 2001 Open channel flow resistance. *Journal of Hydraulic Engineering* **128**, 20–39.

Zhang, X. Q., Bao, W. M., Yu, Z. B. & Qu, S. M. 2009 Real-time correction on the river stage forecasting with an equivalent stage approach. *Hydroinformatics in Hydrology, Hydrogeology and Water Resources.* IAHS Publication **331**, 275–283.

First received 18 October 2011; accepted in revised form 11 September 2012. Available online 11 December 2012